Penetrant diffusion in frozen polymer matrices: A finite-size scaling study of free volume percolation

H. Weber* and W. Paul
Institut für Physik, Johannes-Gutenberg-Universität, Staudingerweg 7, D-55099 Mainz, Germany
(Received 7 February 1996)

The diffusion of penetrant particles in frozen polymer matrices is investigated by means of Monte Carlo simulations of the bond fluctuation model. By applying finite-size scaling to data obtained from very large systems it is demonstrated that the diffusion process takes place on a percolating free volume cluster describable by a correlated site percolation model which falls into the same universality class as random percolation. The diverging correlation length entails a pronounced dependence of the diffusion constant on the size of the simulated system. It is shown that this dependence is appreciable for a wide range of parameters around the transition. [S1063-651X(96)05810-2]

PACS number(s): 61.25.Hq, 66.30.−h, 64.60.Ak, 61.43.Fs

I. INTRODUCTION

The knowledge of the diffusion constant of small penetrant molecules in polymers is of crucial importance for many technological applications, such as the design of barrier materials, filters and gas-separating membranes, or the controlled release of drugs [1–3]. In general, the diffusion constant is strongly dependent on the chemical species both of the diffusant and the matrix material. The choice of suitable materials, as well as the design of new matrix substances, would be greatly facilitated if it were possible to predict macroscopic transport properties from the chemical composition of the materials. Various theoretical models have been developed that aim to describe the transport of small molecules through polymers, see Refs. [1–4] for reviews. However, these approaches either do not incorporate the structural details of the polymers on an atomistic level, or they rely on model parameters that cannot be determined within the framework itself.

Computer simulations, on the other hand, provide the opportunity, at least in principle, to compute transport properties directly from the microscopic structure of the substances involved. Molecular dynamics simulations [5–13] and simulations based on transition state theory [14,15] have been successful in reproducing the qualitative dependence of the diffusion behavior on the size of the penetrant and on the chemical structure of the matrix. Absolute values of the diffusion constants, however, appear to be much harder to reproduce.

To some extent this may be attributed to an insufficient knowledge of the correct parametrization of the force fields used in the modeling of the investigated substances. Secondly, there may be difficulties in obtaining a sufficient disorder average. Chemically detailed simulations typically only have access to a very limited number of independent sample configurations of rather small size of the order of 30 Å, and strong statistical variations can be observed between configurations, see, e.g., Ref. [15].

Thirdly, it is conceivable that systematic errors occur as a result of the finite size of the simulated systems. There appears to be a tendency for simulations to overestimate the diffusion constant [5,6,8–10]. One possible explanation for this is the following. The mean square displacement $\langle R^2\rangle(t)$ of the penetrant particles typically shows a crossover from a regime of anomalous diffusion with a diffusion exponent $\alpha<1$ at intermediate times to a regime of normal diffusion with $\alpha=1$ at large times [9,14,15]. The diffusion exponent α is defined by

$$\langle R^2\rangle \propto t^{\alpha}. \tag{1}$$

In the atomistically detailed simulations this crossover typically occurs when the penetrant has on average diffused over a distance comparable to the size L of the simulation box, regardless of temperature or penetrant species. Clearly, diffusion must necessarily become normal as, due to the periodic boundary conditions that are applied, the particle begins to average over the periodic images of the simulation box. It is therefore to be expected that in these studies the crossover to normal diffusion was induced by the periodic boundary conditions and does not reflect the true physical properties of the matrix. In a larger system the crossover length scale would have been larger, which would have resulted in a smaller value of the measured diffusion constant.

For these reasons it would be desirable to (a) identify the physical mechanism that gives rise to anomalous diffusion in these systems, and (b) determine the true physical crossover length as a function of external parameters such as temperature and polymer density. To this end it is necessary to systematically vary the system size, and to simulate much larger systems. Also, a large number of statistically independent configurations are necessary to obtain a sufficient disorder average if the regimes of anomalous and normal diffusion are to be identified unambiguously. Neither molecular dynamics nor transition state theory based simulations are presently capable of meeting these requirements.

In the present paper we therefore address the above questions in a simplified model. The first simplification we introduce is to sacrifice chemical detail and simulate a coarse-grained lattice model that describes the universal physical

*Electronic address: hweber@chaplin.physik.uni-mainz.de

properties of a whole class of polymeric materials. We have carried out Monte Carlo simulations of the bond fluctuation model [16,17] which achieves a high degree of efficiency while at the same time allowing for a large number of polymer conformations thus providing a close approximation to the continuous case. With this model, large polymer melt configurations were generated and thoroughly equilibrated at a variety of temperatures, densities, and system sizes.

As a further simplification, we then froze all polymer degrees of freedom before penetrants were inserted and the penetrant diffusion behavior was monitored. Experimentally, this corresponds to a sudden deep quench of the system from its equilibration temperature to a temperature where penetrants are still mobile but penetrant mobility is decoupled from the mobility of the matrix. We thus assume a complete separation of polymer and penetrant time scales. The frozen-in matrix is taken as an approximation of the glassy state of the polymer where virtually no rearrangement is possible on the time scale of observation [18].

This approach allows us to generate a large number of well equilibrated and statistically independent sample configurations of very large sizes that could not be obtained otherwise. From a thorough finite-size scaling study of this simple system important insights can be gained which are likely to be of relevance for a proper appreciation of finite-size effects in the simulation of more realistic polymer-penetrant systems.

Our theoretical considerations and numerical results can be summarized as follows. Long-time diffusion in a frozen matrix is possible only if the free volume of the matrix percolates. The polymer matrix undergoes a percolation transition which can be temperature or density driven. Measurement of the critical exponent ratios confirms that the transition falls into the universality class of conventional random percolation. The length scale of the crossover from anomalous to normal diffusion increases dramatically as the transition is approached. In matrices *at* the percolation transition penetrant diffusion is anomalous on all length scales. A large crossover length entails a pronounced dependence of the diffusion constant on the system size. Our simulations show that at fixed polymer volume fraction ϕ the crossover length is appreciable, and thus finite-size effects are likely to occur, for a wide range of temperatures around the transition.

The paper is organized as follows. The bond fluctuation model is described in Sec. II. In Sec. III we give a theoretical analysis of the diffusion of penetrant particles through frozen polymer matrices. This analysis is verified by computer simulations the results of which are presented in Sec. IV. A summary and outlook are given in Sec. V.

II. MODEL

In the present study the bond fluctuation model [16,17] is used to describe the polymer matrix and the penetrants. It is constructed on a simple cubic lattice in three dimensions. Periodic boundary conditions are applied throughout. Figure 1 shows a projected schematic representation. Polymers are modeled as chains of effective monomers. In this study, the number of effective monomers per chain was chosen to be $N=20$. Each effective monomer consists of a cube of eight lattice points. Effective monomers interact with each other via excluded volume interactions. The excluded volume per monomer is $(2a)^3$ where a is the lattice constant. Each effective monomer of this coarse-grained model corresponds to a piece of a chemical realistic chain consisting of about five backbone bonds [19,27], i.e., to a length of roughly 5 Å.

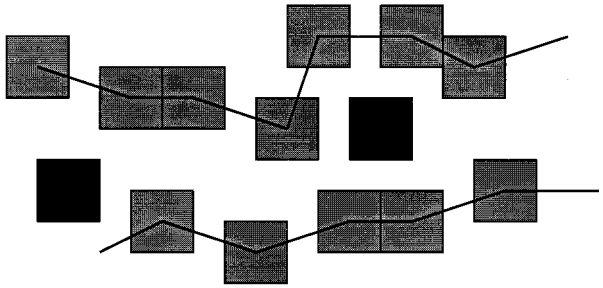

FIG. 1. Bond-fluctuation model (schematic projected representation). Gray squares denote effective monomers of the polymer chains, and black squares denote penetrant particles.

Along the chains adjacent molecules are connected by bonds which are chosen from a restricted set of bond vectors comprising the following classes of vectors: [2,0,0], [2,1,0], [2,1,1], [2,2,1], [3,0,0], [3,1,0]. The square brackets denote all possible permutations and sign inversions of the components. The set of allowed bond vectors was chosen such as to make a crossing of bonds impossible in the course of the random hopping dynamics of the monomers. The bond crossing constraint is thus implemented implicitly and need not be checked during the simulation. The chosen set of bond vectors contains 108 vectors of five different lengths and allows for 87 different bond angles and therefore represents a close approximation to the continuous case. The range of available bond lengths $2 \leqslant b \leqslant \sqrt{10}$ mirrors the fluctuations in the end-to-end distance of a subchain in a real polymer which are due to its torsional degrees of freedom. More details on the ''philosophy'' of the model are given in Ref. [19].

This model, athermal or in combination with a suitable Hamiltonian, has recently been successfully applied to the simulation of single chains [16], statics and dynamics of polymer melts [20], polymer mixtures [21,22], wetting phenomena [23], polymer brushes [24], block copolymers [25], and the glass transition in polymers [26]. Although the model does not represent any information on the smallest length scales present in chemical polymers, it faithfully reproduces their universal medium and large scale properties. In particular, the model has been shown to reproduce well the static properties of dense polymer melts [20].

Preliminary studies showed qualitatively that penetrant diffusion possesses a pronounced dependence on the stiffness of the polymer chains. In order to investigate this effect more systematically the following Hamiltonian was introduced

$$\mathcal{H}(\{b\},\{\theta\}) = \sum_{\text{bonds}} \epsilon_b (b-b_0)^2 + \sum_{\text{angles}} \epsilon_\theta \cos\theta (1+c_0 \cos\theta). \tag{2}$$

The temperature (energy) scale is fixed by setting ϵ_b to unity. The values of the remaining parameters were set to $b_0=0.86$, $\epsilon_\theta=0.67$, and $c_0=0.03$ which leads to a favoring

of short bonds and stretched chains. The choice of these values was guided by experience gained by mapping the bond fluctuation model onto chemically realistic polymers [19,27].

We have simulated systems of a linear dimension of up to $L=190$ lattice constants. According to general expectations from the mapping onto realistic polymers [19,27] this corresponds to sizes of up to roughly 400 Å. The largest of these systems consisted of around 430 000 monomers. The simulation of systems of this size is constrained by high demands on both computer memory and the computing time required to equilibrate and propagate the systems. The present study required a total of about one thousand CPU hours on an IBM RS 6000/370 workstation.

Polymer matrices are prepared in the following way. Using the configurational bias algorithm [28] polymers are stochastically grown into the simulation box athermally but subject to excluded volume constraints until the desired density has been reached. The temperature is then set to the desired value T and the sample is equilibrated in the canonical ensemble using the slithering snake algorithm [29]. Thorough equilibration is ensured by propagating the systems for ten times the time required for the radius of gyration to reach its equilibrium value. Depending on the system size, up to one thousand statistically independent configurations per system size are generated to ensure good statistical averaging. Configurations are assumed to be statistically independent for the purposes of the static percolation analysis after propagation of the chains over several radii of gyration. Propagation is carried out either canonically or grand canonically. During grand-canonical simulations the configurational bias algorithm [28] is used for chain insertion and deletion in order to achieve appreciable acceptance rates.

The polymer configurations thus generated are then *quenched* to absolute zero, i.e., all polymer degrees of freedom are frozen in. The frozen configurations are subjected to two types of analysis: (i) a static analysis of the free volume accessible to the penetrant, and (ii) diffusion of penetrant particles through the matrix. These analyses will be described in more detail below. No polymer motion takes place during any part of the analysis.

Penetrants are modeled as cubes of eight lattice sites, i.e., the same size as an effective monomer. They interact with the polymer matrix solely through excluded volume interactions. As shown below, these monomer penetrants typically exhibit a distinct regime of anomalous diffusion. Penetrants are inserted only into free volume clusters that percolate. This scenario was chosen because glassy polymer membranes can only be permeated along percolating clusters.

We have also considered another type of penetrant which occupies only a single lattice site, but for these penetrants no appreciable regime of anomalous diffusion could be detected. This demonstrates that not only the quantitative, but also the qualitative diffusion behavior strongly depends on the size of the penetrant. Since in the present context we are mainly concerned with the role of anomalous diffusion we will in the remainder of the paper concentrate on monomer penetrants only.

III. THEORETICAL BACKGROUND

Penetrant diffusion is modeled as a random walk along the static free volume between the polymers. The free volume of the matrix consists of distinct clusters, and during the entire walk each penetrant particle is confined to the cluster on which it started. The diffusion behavior is, therefore, determined by the static percolation properties of the free volume clusters. The occupied sites in the conventional site percolation problem correspond to the sites of free volume between the polymer chains that are accessible to the penetrants. At fixed equilibration temperature T the free volume should undergo a percolation transition as a function of the density. Expressed in terms of the volume fraction ϕ occupied by the polymer chains, the free volume should percolate for volume fractions *below* a critical value ϕ_c.

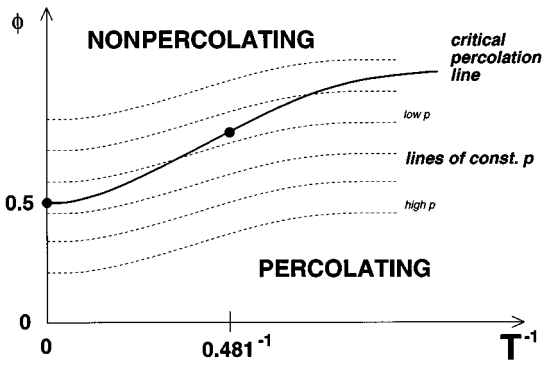

FIG. 2. Schematic phase diagram of free volume percolation in the inverse temperature—volume fraction plane. The fine dashed lines are lines of constant free volume, which corresponds to the occupation probability p in conventional percolation. The filled circles mark the two critical points determined quantitatively by simulation.

However, in contrast to conventional site percolation, the spatial arrangement of the sites is not random. The presence of the polymer chains leads to local correlations between the sites of free volume: the sites are locally aligned due to the connectivity of the chains. In this way, channels are formed which should facilitate percolation as compared to the random case.

Comparing polymer configurations of the same polymer volume fraction ϕ but of different equilibration temperatures T, a lower temperature will lead to stiffer chains and thus to more pronounced channels of free volume. This, in turn, should result in a greater chance of finding a percolating cluster. For fixed polymer volume fraction ϕ the free volume should thus undergo a *temperature*-driven percolation transition with the percolating phase located at $T<T_c$.

The phase diagram of this percolation problem in the (T,ϕ) plane should therefore consist of a critical percolation line separating a percolating phase at low values of T and ϕ and a nonpercolating phase at high values. In other words, the critical polymer volume fraction ϕ_c should be a decreasing function of the equilibration temperature T. A schematic representation of the expected phase diagram is shown in Fig. 2.

The correlations between the sites are expected to be of finite range related to the excluded volume correlation length in the melt [30]. On larger length scales two monomers have no apparent memory of belonging to the same chain which leads to the well-known Gaussian behavior of chains in the melt. Therefore, the present correlated percolation scenario should fall into the same universality class as conventional

random percolation. The present situation is in close analogy to percolation of correlated Ising clusters in the paramagnetic phase [31,32].

The central signature of a percolation transition is the power-law divergence of the percolation correlation length ξ, which is defined [33] via the exponential decay of the pair connectedness function, or, equivalently, as the average distance of two sites belonging to the same cluster. As the percolation point is approached, ξ diverges with some exponent ν

$$\xi \propto |\epsilon|^{-\nu},$$

where ϵ is a suitable parameter expressing the separation from the transition; usually, $\epsilon = p - p_c$. One important consequence of this divergence is the particular behavior of observables in systems of finite size L, which is described by finite-size scaling [33–35]. For an observable x whose behavior near the percolation point in the infinite system is described by some critical exponent χ through

$$x \propto |\epsilon|^{\chi},$$

the finite-size scaling relation reads

$$x(L,\xi) \propto \xi^{-\chi/\nu} X\left(\frac{L}{\xi}\right). \tag{3}$$

X is the scaling function for x which tends to unity for $L/\xi \to \infty$, and tends to $(L/\xi)^{-\chi/\nu}$ for $L/\xi \to 0$. For a finite system at the critical point, where $L/\xi = 0$, we thus have

$$x(L,\xi) \propto L^{-\chi/\nu}. \tag{4}$$

Once a transition point has been located, this relation can be used to check whether finite-size scaling holds, and thus to obtain evidence of a second-order phase transition. It can also be used to determine the critical exponent ratio χ/ν for observable x. Critical exponent ratios obtained in this way provide evidence of the universality class of the transition. In the percolation case, suitable observables for this type of analysis are the percolation probability P, i.e., the fraction of sites that are part of a percolating cluster, which is the order parameter of the percolation transition, and the average cluster size S, which plays the role of the susceptibility. Their critical exponents are denoted β and $-\gamma$, respectively. Note that S is defined such as to include only contributions from nonpercolating clusters [33].

Furthermore, for an observable x with critical exponent $\chi = 0$, relation (4) reduces to $x(L,\xi) = \text{const}$. This implies that curves of x as a function of a control parameter such as T or ϕ, plotted for different system sizes L, should all intersect in a single intersection point at the critical value of the control parameter. Such a plot is a very sensitive test of the divergence of the correlation length ξ, and furthermore provides an accurate tool for the location of the transition point. One class of observables with exponent $\chi = 0$, which have frequently been used in this way, are the cumulants of the order parameter and the energy, see, e.g., Ref. [36]. In the case of percolation, a generic observable with $\chi = 0$ is the spanning probability P_s which is defined as the probability for a configuration to contain at least one percolating cluster. Its critical exponent is zero since in the infinitely large system P_s possesses a discontinuous jump at the transition point from $P_s = 0$ in the disordered phase to $P_s = 1$ in the percolating phase [35]. Thus measurements of $P_s(T)$ and $P_s(\phi)$ for a range of system sizes L make it possible to provide evidence for the phase diagram suggested above.

The percolation analysis just given has the following implications for the diffusion behavior of the penetrant molecules. Percolation clusters have fractal structure on length scales smaller than the correlation length ξ, and are Euclidean (homogeneous) on larger length scales [37]. Consequently, diffusion on percolation clusters is anomalous on short length and time scales, and normal on long scales [38,39]. The same type of behavior should therefore be expected for the present model. The crossover length R_{cross} separating the two regimes should scale as the percolation correlation length ξ, see Ref. [33]. This implies that as the parameters T and ϕ are varied such as to approach the critical percolation line, R_{cross} will increase without bound. In a system right at criticality, diffusion will be anomalous on all length scales. In a simulation of a system of given size L there will thus always be a range of values of T and ϕ for which the true physical crossover length R_{cross} exceeds the system size, and where the crossover will occur prematurely when the mean square displacement becomes of the order of the system size. An estimate of the width of this region, and thus of the importance of this effect, has been obtained by simulations of the penetrant dynamics to be described below.

IV. NUMERICAL RESULTS

A. Static analysis

On the basis of the above finite-size scaling considerations we have first carried out a static percolation analysis of large numbers of polymer configurations of different system sizes in the range $L = 31, \ldots, 190$. In each configuration we identify all clusters of free volume accessible to the penetrant and determine which of these clusters percolate. Percolating clusters are required to satisfy periodic boundary conditions. The spanning probability P_s, the percolation probability P and the average cluster size S, all defined in the preceding section, are calculated as averages over statistically independent configurations.

In a first series of simulations we generated polymer configurations in the canonical ensemble at the following values of the equilibration temperature (in units of ϵ_b): $T = 0.415, 0.439, 0.470, 0.502, 0.533$. The polymer volume fraction was kept constant at $\phi = 0.5$. At this volume fraction, the polymer systems possesses the characteristics of a dense melt [20]. A plot of the measured spanning probability $P_s^{(L)}(T)$ as a function of temperature for various system sizes L is shown in Fig. 3. The curves for different L clearly intersect in a common intersection point. From the abscissa of this intersection point we obtain a transition temperature (at $\phi = 0.5$) of $T_c = 0.481 \pm 0.001$. Figure 4 shows that the spanning probabilities at $T = 0.481$ are independent of system size within statistical errors. Figures 3 and 4 provide strong evidence of a diverging correlation length, and thus of a second-order phase transition.

Having determined the transition temperature we then generated and analyzed further configurations of different

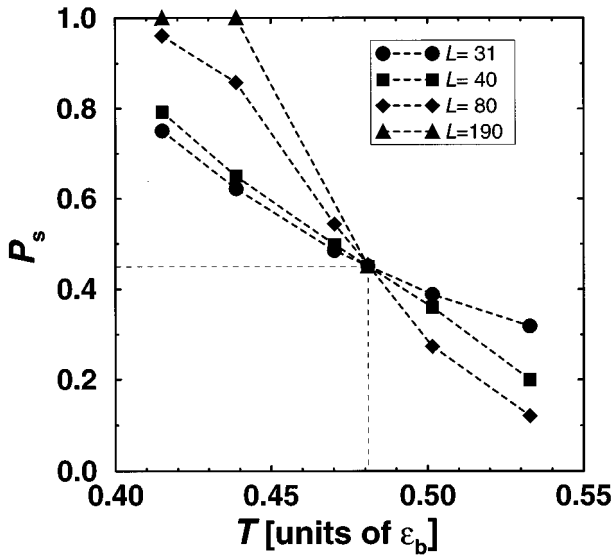

FIG. 3. Spanning probability P_s as a function of temperature for various system sizes L. The polymer volume fraction is $\phi=0.5$. The temperature scale is set by the parameters of the Hamiltonian.

system sizes at T_c. Double-logarithmic plots of the percolation probability P and the average cluster size S as functions of the system size are shown in Fig. 5. The data are well described by power laws according to (4). Least-squares fits yield estimates of the critical exponent ratios $\beta/\nu=0.46\pm0.01$ and $\gamma/\nu=2.1\pm0.1$. Within errors, the measured exponent ratios agree with the theoretical values for random percolation in three dimensions, $\beta/\nu=0.466$ and $\gamma/\nu=2.05$, cf. Ref. [33]. These findings support the expectation that the present correlated free volume percolation scenario falls into the same universality class as random percolation. Note that a significant reduction of the error, or a determination of the absolute values of β, γ, and ν would require a computational effort very much larger than in the

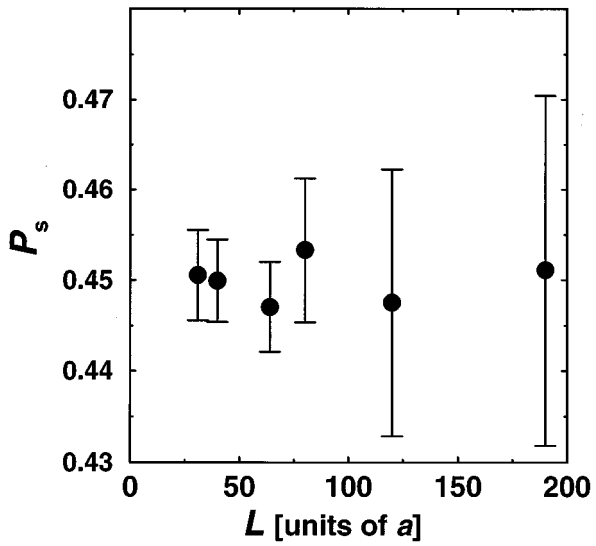

FIG. 4. Spanning probability P_s as a function of system size L at $(T=0.481,\phi=0.5)$. a is the lattice constant.

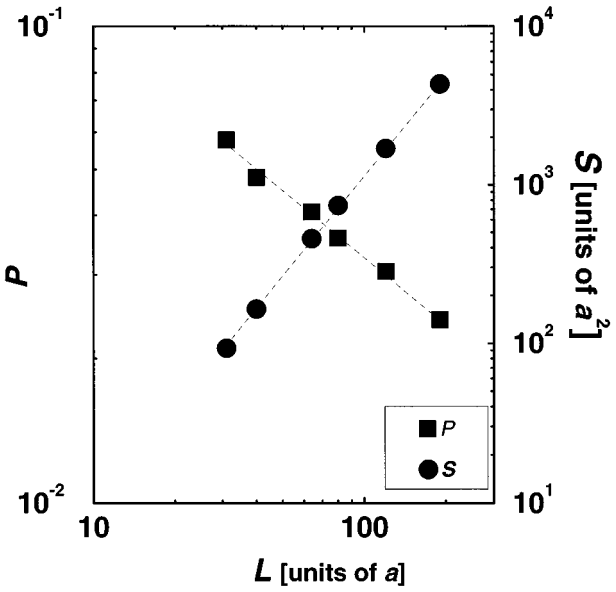

FIG. 5. Percolation probability P (order parameter) and average cluster size S (susceptibility) at the critical point $(\phi=0.5,T=0.481)$ as functions of system size L. a is the lattice constant. The dashed lines denote the results of least squares fits to a power law.

case of random percolation, due to the high cost of generating statistically independent polymer configurations.

We then carried out a second series of simulations in order to determine the critical polymer volume fraction ϕ_c in the athermal system $T=\infty$. The knowledge of this value is useful both as a reference point for comparison with other percolation scenarios and in order to check the prediction of Sec. III that the critical volume fraction decreases with increasing equilibration temperature. Again, the intersection method was used to determine ϕ_c. The chosen system sizes were $L=40$, 64, 80, and 110. For each system size a single simulation is sufficient to obtain P_s as a function of ϕ if the simulation is carried out at constant chemical potential μ and constant volume, and the joint histogram $H_\mu(P_s,N)$ is recorded. The histogram $H'_\mu(P_s,N)$ at a different value of the chemical potential μ' can then be calculated without further simulation by reweighting the measured histogram with $\exp\{(\mu'-\mu)N\}$ and renormalizing the result [40]. From this, $\langle\phi\rangle$ and P_s are obtained by summation.

One drawback of the histogram reweighting technique is that for the large systems necessary to reach the scaling regime the density fluctuations become small, and, hence, the chemical potential or density range over which extrapolation is reliable is rather limited (note that the more sophisticated multihistogram method goes some way towards alleviating this problem [17]). The simple histogram method requires some rough knowledge of the value of the critical chemical potential. This is the reason why separate simulations were carried out for each temperature during our first series of simulations at constant polymer volume fraction ϕ. In order to obtain an estimate of a suitable value of the chemical potential for the second simulation series we assumed that the value of $P_s(\xi=\infty)$ is universal, i.e., that it is the same for all critical points along the percolation line. This should be true under the finite-size scaling assumption [34] since all

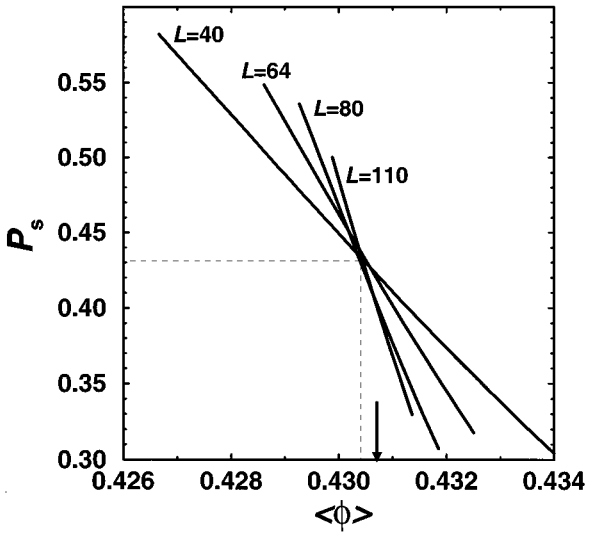

FIG. 6. Spanning probability P_s at $T=\infty$ as a function of the polymer volume fraction ϕ for various system sizes L. a is the lattice constant. Both quantities are obtained by histogram extrapolation. The vertical arrow marks the value of $\langle\phi\rangle$ at which the simulation was carried out.

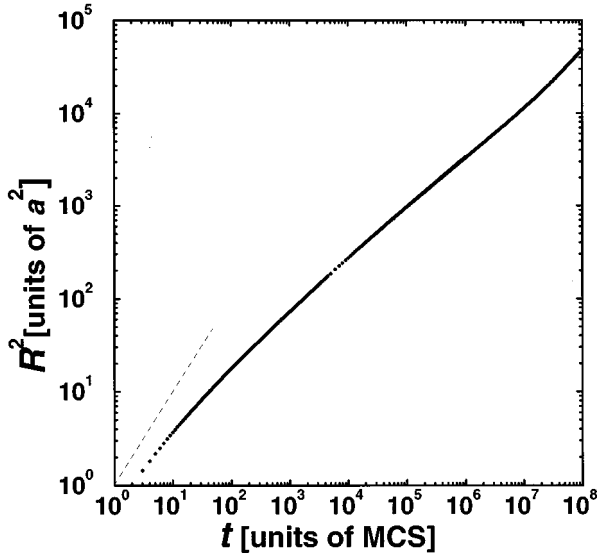

FIG. 7. Mean square displacement R^2 of penetrant particles at the critical point ($\phi=0.5, T=0.481$) as a function of time t. a is the lattice constant. The dashed line has slope unity.

these critical points can be expected to belong to the same universality class. We carried out a brief preliminary simulation of a small system with large fluctuations, extrapolated, and read off the chemical potential at which P_s had the value observed at the intersection point in the first series. This value was then used for the simulation of the various larger systems. The results are shown in Fig. 6. The vertical arrow marks the average density during the simulation. The figure shows that our assumption indeed provided a reasonable estimate of the critical density. The values obtained for P_s in the first and the second series, 0.45 ± 0.02 and 0.43 ± 0.03 agree within errors.

Again, it is observed in Fig. 6 that all curves intersect in a common point to high accuracy. For the critical polymer volume fraction in the athermal system we obtain the value $\phi_c(T=\infty)=0.4304\pm0.0003$. The finite-size scaling analysis therefore allows us to determine this value with a relative error of less than 10^{-3}.

Both critical points thus determined ($T=0.481, \phi=0.5$) and ($T=\infty, \phi=0.4304$) are marked as filled circles in the schematic percolation phase diagram of Fig. 2.

B. Penetrant diffusion

We now turn to the numerical analysis of penetrant diffusion. In order to give further support to our percolation analysis we measured the mean square displacement of the penetrants in polymer matrices *at* the critical point ($\phi=0.5, T=0.481$). The linear dimension of the samples was $L=190$. Three separate sets of walks were carried out to obtain approximately the same resolution on all time scales. We used 120 statistically independent polymer configurations each for the short and the medium length walks, and 55 independent configurations for the long walks. Each configuration contained 50 penetrant particles. The penetrant mean square displacement is shown double logarithmically as a function of time in Fig. 7, and its logarithmic derivative

$$\alpha(t)=\frac{d\ \log\langle R^2\rangle}{d\ \log t}, \tag{5}$$

sometimes called the ''local diffusion exponent'' [41,42], is shown in Fig. 8.

On the very shortest time scales $t<10$ the curve has a slope of approximately unity, see Fig. 7. This is due to the free diffusion of penetrants within the locally Euclidean cavities of the polymer matrix. With increasing time the slope of the curve decreases, and the mean square displacement crosses over to a regime of anomalous diffusion due to the fractal structure of the free volume percolation cluster. The crossover between these two regimes is very gradual and extends over more than five decades in time. This can be rationalized by assuming that on length scales of roughly $O(10)$ lattice constants the penetrant may have explored a ramified free volume cluster but has not yet been forced to retrace its path due to dead ends along the branches of the cluster. Only after visiting enough dead ends of sufficiently varying lengths the fractal nature of the percolating free volume cluster becomes noticeable, leading to the anomalous diffusion of the penetrant particle [43].

For times between $t\approx4\times10^5$ MCS (Monte Carlo sweeps) and $t\approx5\times10^6$ MCS the local diffusion exponent $\alpha(t)$ assumes a plateau value, showing that the true value of α in the infinitely large system has been reached. The height of the plateau is

$$\alpha=0.532\pm0.002. \tag{6}$$

This value agrees very well with the best known value of $\alpha=0.533\pm0.027$ for conventional random percolation in three dimensions, with diffusion taking place on percolating clusters only [42]. This finding gives strong additional sup-

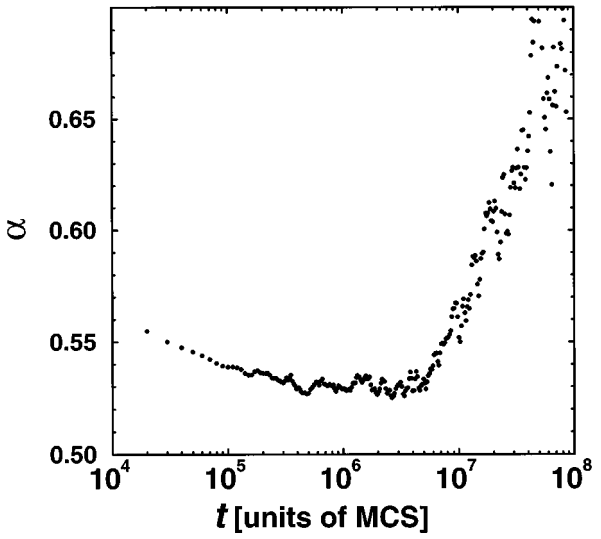

FIG. 8. Local diffusion exponent α (logarithmic derivative of the mean square displacement) at the critical point ($\phi=0.5, T=0.481$).

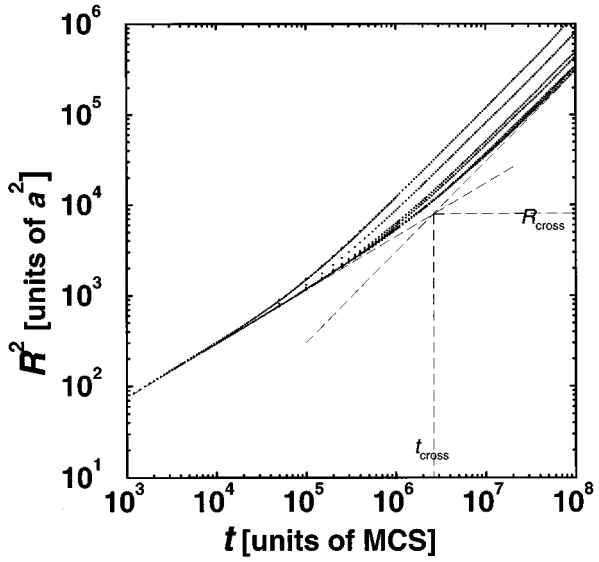

FIG. 9. Mean square displacement R^2 of penetrant particles at ($\phi=0.5, T=0.415$), i.e., off criticality, for various system sizes L, as a function of time t. From top to bottom, the curves correspond to system sizes $L=31,40,61,72,86,120,190$. The last three curves virtually coincide. a is the lattice constant.

port to our percolation analysis. Finally, for times larger than $t\approx 5\times 10^6$ MCS a second crossover occurs back to normal diffusion. This is primarily induced by the periodic boundary conditions, but it may also be due to a finite crossover length since the critical temperature was known only approximately. Note that the chosen system size of $L=190$ was just sufficient for the plateau to become visible.

The relative magnitudes of the crossover length R_{cross} and the system size L control the extent to which measured diffusion constants are subject to finite-size effects. It is thus of interest to know in absolute terms how far away from the transition R_{cross} becomes appreciable. We have therefore carried out a further simulation series in order to determine the absolute value of the crossover length R_{cross} at a state space point well off the transition. We chose a polymer volume fraction of $\phi=0.5$ and a temperature of $T=0.415$. We measured the penetrant mean square displacement in systems of different sizes L and determined the size-dependent crossover length scale $R_{\text{cross}}^{(L)}$. The crossover length scale in the thermodynamic limit was estimated by increasing the system size until $R_{\text{cross}}^{(L)}$ was clearly size independent. A maximum system size of $L=190$ was used in order to obtain unambiguous results. The measured mean square displacements are shown in Fig. 9. They show the same qualitative behavior as observed in other simulations, cf., e.g., Ref. [14]. From the mean square displacement, the crossover point was determined as the intersection point of straight lines fit to the curve in the anomalous and the diffusive regimes, respectively, see Fig. 9. The diffusion constant was obtained according to

$$D=\lim_{t\to\infty}\frac{\langle R^2\rangle}{6t}. \tag{7}$$

The resulting crossover lengths and diffusion constants are shown in Figs. 10 and 11, respectively. Both quantities exhibit a pronounced size dependence for system sizes $L<80$. In this regime, the crossover length scale R_{cross} is to very good approximation equal to the system size L, which provides strong evidence that for these small systems the anomalous-to-normal crossover is induced by the periodic boundary conditions. For system sizes $L\geqslant 80$, on the other hand, R_{cross} and D are virtually size independent. In these large systems the diffusion behavior directly reflects the structure of the percolating cluster. However, a weak residual size dependence can be observed even for $L\geqslant 80$ because the

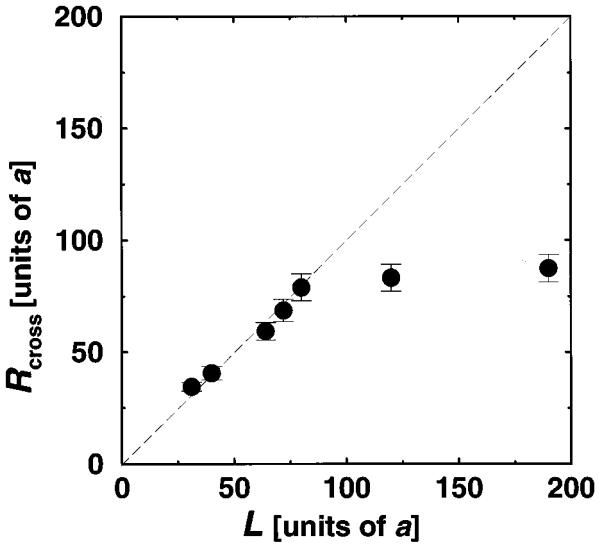

FIG. 10. Crossover length R_{cross} at ($\phi=0.5, T=0.415$) as a function of system size L. R_{cross} was determined from the intersection of straight lines fit to $R^2(t)$ in the anomalous and the normal regimes, see Fig. 9. The dashed line marks $R_{\text{cross}}=L$. a is the lattice constant.

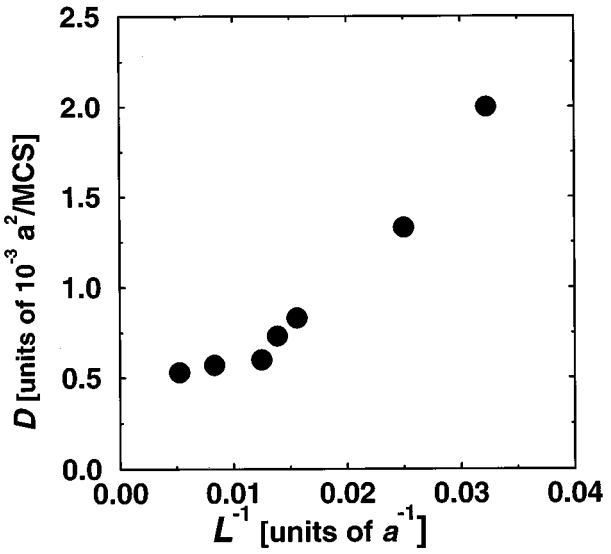

FIG. 11. Diffusion constant D at ($\phi=0.5, T=0.415$) as a function of inverse system size L^{-1}. a is the lattice constant. Errors are smaller than the size of the symbols.

percolation correlation length ξ, which controls the crossover length R_{cross}, is itself subject to finite-size rounding. In the finite systems, ξ is smaller than in the thermodynamic limit, and it increases with increasing system size. This effect is still remarkably strong even for the large systems investigated. We measured $\xi=16.9\pm0.1$ for $L=80$, and $\xi=23.4\pm0.1$ for $L=190$. This accounts qualitatively for the observed residual dependence of R_{cross} on L.

The fact that at the investigated state space point ($T=0.415, \phi=0{,}5$), i.e., about 15% below the transition temperature, the crossover length in the thermodynamic limit is still of the order of 80 lattice constants implies that over a large part of the phase diagram very large systems, and thus significant computing resources, are required for a correct determination of the diffusion constant.

V. DISCUSSION

In this paper we analyzed in detail the reason for the occurrence of anomalous penetrant diffusion in polymer matrices as seen in a variety of atomistic modeling attempts of gas permeation through polymer membranes. Usually in these situations one is interested in the permeation properties of glassy membranes. This question therefore typically involves a separation of matrix and penetrant time scales. In order to investigate the effects of finite system size on the extent of the anomalous diffusion regime and to ensure sufficient disorder averaging we chose to study a simple and computationally efficient lattice model which nonetheless captures the essential physics. With the separation of time scales in mind the polymer matrix was completely frozen for computational expedience. In this limit the penetrant diffusion is a dynamic analysis of the geometry of the free volume. We analyzed in detail and with high statistical accuracy the finite-size scaling behavior of the free volume percolation problem and showed that it belongs to the universality class of random percolation. The diffusion exponent in the subdiffusive regime of the mean square displacement of the penetrants was shown to be equal to the value known from diffusion studies of three dimensional random percolation.

In contrast to random site occupancy the free volume in the polymer matrix is locally correlated due to the connectivity and stiffness of the surrounding chains. This correlation is of small spatial range and can be controlled by a Hamiltonian for the intramolecular degrees of freedom that changes the chain stiffness as a function of temperature. This leads to a critical line in the percolation phase diagram in the temperature-density plane. For the density and energy parameters investigated the percolation transition occurred in the fluid phase of the model, well separated from the glass transition. As the two phenomena depend on temperature and density in different ways this need not be true for all parameter choices. In general, however, we are here dealing with two distinct phenomena. E.g., in the present model the free volume percolates at temperatures below the percolation transition, while in the free volume theory of the glass transition the liquidlike clusters of (polymer) particles percolate at temperatures above the glass transition.

The bond fluctuation lattice model is known to represent well the universal static properties of polymer melts. The percolation analysis is conceptually not confined to the lattice case. Various models of percolation in continuous space have been investigated; for an overview see Ref. [44]. While the static continuum percolation exponents have been shown to be equal to their lattice counterparts [45], the dynamic exponents differ. Their precise values depends on the choice of the continuum model [46]. In particular, the ''Swiss cheese'' model [45,46] would be suited to describe the percolation of the free volume between the monomers of a bead-spring polymer model in continuous space. In the ''Swiss cheese'' model the anomalous diffusion exponent α is about 13% smaller than in the 3D lattice case [46]. Thus the effect of anomalous diffusion will be even more pronounced in a continuum model. The qualitative picture obtained in our study is thus not an artefact of the choice of a lattice model.

Our simulations apply directly to real systems if studied at constant volume. In a constant pressure experiment the increase in stiffness upon lowering the temperature will be counteracted to some degree by the thermal expansion of the system. More important though is the effect of matrix mobility which changes the percolation problem from a static to a dynamic one. In this case we expect a crossover from a low temperature regime where matrix mobility is low and the penetrant diffusivity is dominated by the static properties of the matrix, to a high temperature regime where the fluctuations of the matrix dynamically homogenize the environment sampled by the penetrant, and penetrant diffusivity is coupled to the dynamics of the matrix. At intermediate temperatures we expect a rounded maximum of the crossover length scale separating anomalous from normal penetrant diffusion. It is in this temperature region that the anomalous diffusion seen in experiments [47] and atomistic simulations will be most pronounced. These issues will be analyzed in detail in a forthcoming publication [48].

ACKNOWLEDGMENTS

It is a pleasure to thank K. Binder for many stimulating discussions, and M. Müller for help with technical aspects of

the simulation. This work was carried out as part of a EU Joint Research Project under Grant No. CIPA-CT93-0105. We gratefully acknowledge discussions with the other members of this project, in particular, P. Argyrakis, D. W. Heermann, and A. Milchev. The study was made possible by a generous grant of computing time on the SC 900 parallelcomputeroftheRegionaleHochschulrechenzentrumKaiserslautern.

[1] J. Crank and G. S. Park, *Diffusion in Polymers* (Academic, London, 1968).
[2] J. Comyn, *Polymer Permeability* (Chapman and Hall, London, 1985).
[3] W. R. Vieth, *Diffusion in and through Polymers* (Hanser, München, 1991).
[4] H. L. Frisch, CRC Crit. Rev. Solid State Mater. Sci. **11**, 123 (1983).
[5] R. M. Sok, H. J. C. Berendsen, and W. F. van Gunsteren, J. Chem. Phys. **96**, 4699 (1992).
[6] F. Müller-Plathe, J. Chem. Phys. **96**, 3200 (1992).
[7] F. Müller-Plathe, S. C. Rogers, and W. F. van Gunsteren, Chem. Phys. Lett. **199**, 237 (1992).
[8] F. Müller-Plathe, S. C. Rogers, and W. F. van Gunsteren, Macromolecules **25**, 6722 (1992).
[9] F. Müller-Plathe, S. C. Rogers, and W. F. van Gunsteren, J. Chem. Phys. **98**, 9895 (1993).
[10] R. H. Boyd and P. V. Krishna Pant, Macromolecules **24**, 6325 (1991).
[11] P. V. Krishna Pant and R. H. Boyd, Macromolecules **25**, 494 (1992).
[12] P. V. Krishna Pant and R. H. Boyd, Macromolecules **26**, 679 (1993).
[13] J. Han and R. H. Boyd, Macromolecules **27**, 5365 (1994).
[14] A. A. Gusev and U. W. Suter, J. Chem. Phys. **99**, 2221 (1993); **99**, 2228 (1993).
[15] A. A. Gusev, F. Müller-Plathe, W. F. van Gunsteren, and U. W. Suter, Adv. Polym. Sci. **116**, 207 (1994).
[16] I. Carmesin and K. Kremer, Macromolecules **21**, 2819 (1988); in *Polymer Motion in Dense Systems*, edited by D. Richter and T. Springer (Springer, Berlin, 1988); J. Phys. (France) **51**, 915 (1990).
[17] H.-P. Deutsch and K. Binder, J. Chem. Phys. **94**, 2294 (1991).
[18] R. H. Gee and R. H. Boyd, J. Chem. Phys. **101**, 8028 (1994).
[19] K. Binder, *Monte Carlo and Molecular Dynamics Simulations in Polymer Science* (Oxford University Press, New York, 1995), Introduction.
[20] W. Paul, K. Binder, D. W. Heermann, and K. Kremer, J. Phys. (France) **1**, 37 (1991); J. Chem. Phys. **95**, 7726 (1991).
[21] H.-P. Deutsch and K. Binder, Europhys. Lett. **17**, 697 (1992); Macromolecules **25**, 6214 (1992); Macromol. Chem. Macromol. Symp. **65**, 59 (1993).
[22] N. B. Wilding and M. Müller, J. Chem. Phys. **102**, 2562 (1995); M. Müller and N. B. Wilding. Phys. Rev. E **51**, 2079 (1995).
[23] J. S. Wang und K. Binder, J. Chem. Phys. **95**, 8537 (1991); Makromol. Chem. Theory Simulations **1**, 49 (1992); J. Phys. (France) I **1**, 9288 (1991).
[24] J. Wittmer, A. Johner, J. F. Joanny, and K. Binder, J. Chem. Phys. **101**, 4379 (1994).
[25] M. Müller, A. Werner, and F. Schmid, Macromolecules (to be published).
[26] J. Baschnagel, K. Binder, and H.-P. Wittmann, J. Phys. **5**, 1597 (1993); J. Baschnagel and K. Binder, Physica A **204**, 47 (1994); J. Baschnagel, Phys. Rev. B **49**, 135 (1994); P. Ray and K. Binder, Europhys. Letters **27**, 53 (1994).
[27] W. Paul and N. Pistoor, Macromolecules **27**, 1249 (1994).
[28] J. I. Siepmann and D. Frenkel, Molec. Phys. **1**, 59 (1992).
[29] A. D. Sokal, in *Monte Carlo and Molecular Dynamics Simulations in Polymer Science*, edited by K. Binder (Oxford University Press, New York, 1995), and references therein.
[30] P.–G. de Gennes, *Scaling Concepts in Polymer Physics* (Cornell University, Ithaca, 1979).
[31] W. Klein, H. E. Stanley, P. J. Reynolds, and A. Coniglio, Phys. Rev. Lett. **41**, 1145 (1978).
[32] A. Coniglio, H. E. Stanley, and W. Klein, Phys. Rev. Lett. **42**, 518 (1979).
[33] D. Stauffer and A. Aharony, *Introduction to Percolation Theory*, 2nd ed. (Taylor and Francis, London, 1992).
[34] *Finite Size Scaling and Numerical Simulation of Statistical Systems*, edited by V. Privman (World Scientific, Singapore, 1990).
[35] K. Binder and D. W. Heermann, *Monte Carlo Simulation in Statistical Physics* (Springer, Berlin, 1988).
[36] K. Binder, Z. Phys. B **43**, 119 (1981).
[37] H. E. Stanley, J. Phys. A **10**, L211 (1977); R. J. Harrison, G. H. Bishop, and G. D. Quinn, J. Stat. Phys. **19**, 53 (1978); S. Kirkpatrick, *Ill-Condensed Matter*, Les Houches Summer School, edited by R. Maynard and G. Toulouse (North-Holland, Amsterdam, 1979); A. Kapitulnik, A. Aharony, G. Deutscher, and D. Stauffer, J. Phys. A **16**, L269 (1983); B. Sapoval, M. Rosso, J. F. Gouyet, and J. F. Colonna, Solid State Ionics **18/19**, 21 (1986).
[38] Y. Gefen, A. Aharony, and S. Alexander, Phys. Rev. Lett. **50**, 77 (1983).
[39] R. B. Pandey, D. Stauffer, A. Margolina, and J. G. Zabolitzky, J. Stat. Phys. **34**, 427 (1984).
[40] A. M. Ferrenberg and R. H. Swendsen, Phys. Rev. Lett. **61**, 2635 (1988).
[41] S. Havlin and D. Ben-Abraham, Phys. Rev. A **26**, 1728 (1982).
[42] R. B. Pandey and D. Stauffer, Phys. Rev. Lett. **51**, 527 (1983).
[43] J.-P. Bouchaud and A. Georges, Phys. Rep. **4/5**, 127 (1990).
[44] Sh. Feng, B. I. Halperin, and P. N. Sen, Phys. Rev. B **35**, 197 (1987).
[45] W. T. Elam, A. R. Kerstein, and J. J. Rehr, Phys. Rev. Lett. **52**, 1516 (1984).
[46] B. I. Halperin, Sh. Feng, and P. N. Sen, Phys. Rev. Lett. **54**, 2391 (1985).
[47] M. T. Cicerone, F. R. Blackburn, and M. D. Ediger, Macromolecules **28**, 8224 (1995).
[48] H. Weber and W. Paul (unpublished).